Substantial increase in population exposure to multiple environmental burdens in sub-Saharan Africa (2000-2019)

Ankit Sikarwar, Valérie Golaz

ENVIRONMENTAL RESEARCH
LETTERS

LETTER

Substantial increase in population exposure to multiple environmental burdens in sub-Saharan Africa (2000-2019)

Ankit Sikarwar[1,*] and Valérie Golaz[1,2]

[1] Institut national d'études démographiques (Ined), Paris-Aubervilliers, France
[2] LPED, Aix-Marseille Université, Marseille, France
[*] Author to whom any correspondence should be addressed.

E-mail: sikarwar.ankit-kumar@ined.fr

Keywords: multiple environmental burdens, population exposure, sub-Saharan Africa, climate change, air pollution

Supplementary material for this article is available online

OPEN ACCESS

RECEIVED
7 November 2023

REVISED
5 March 2024

ACCEPTED FOR PUBLICATION
25 March 2024

PUBLISHED
9 April 2024

Abstract

In the face of increasing global environmental uncertainties, sub-Saharan Africa stands as a highly vulnerable region with a massive population marked with poverty and inequalities. Moreover, different environmental risk factors can coexist simultaneously as multiple environmental burdens (MEBs); however, population exposure to MEB remains unexamined. Here, using open-access spatial data and critical thresholds, we quantify population exposure to four key environmental risk factors: hazardous fine particulate matter ($PM_{2.5}$) levels, extreme temperature increase, prolonged severe droughts, and green deficit (scarcity of green trees). Further, we explore the concept of MEB, where these risk factors converge. We derive exposure for 2000 and 2019 at the pixel (1 km grid cell) level. We also check how population change, environmental change, and their interaction contribute to the total change in exposure. We found substantial changes in the population exposed from 2000 to 2019, i.e. an increase of ∼460 million people to hazardous $PM_{2.5}$ levels, ∼16 million to extreme temperature increase, ∼13 million to prolonged severe droughts, and ∼246 million to green deficit. Population exposure to at least three of these four environmental risk factors (3EB) has increased by ∼246 million. In this increase in exposure to 3EB, the contribution of environmental change is higher (48%), than that of interaction and population change (36% and 15%, respectively). Notably, there are striking disparities in population exposure, its change, and the contributing effects among countries and regions of sub-Saharan Africa.

1. Introduction

Environmental uncertainties have increased worldwide. Unprecedented episodes of heat waves, droughts, and floods have been striking different regions in recent decades [1]. Half of the global population is exposed to increasing fine particulate matter ($PM_{2.5}$) air pollution [2]. Approximately 420 million hectares of forest loss has been reported due to conversions to other land uses since 1990 [3]. Surging extreme weather events and pollution levels can pose negative consequences for health and well-being. According to the World Health Organization, in 2016, up to 24% of all deaths worldwide were due to adverse environmental conditions [4]. However, these challenges are far from uniform, varying significantly in magnitude and impact at international, national, and subnational scales.

Sub-Saharan Africa remains at higher risk due to intensifying environmental challenges [5]. The literature suggests rising temperature levels [6–8], deteriorating air quality [9], recurring droughts [10, 11], and rampant land use and land cover change [12], among others, as key environmental challenges posing adverse impacts on the health and well-being of over a billion people. The adversities aggregate as much of its population remains below the poverty line, i.e. representing around two-thirds of the global extreme poor population in 2018 [13]. Additionally, many of the countries on the subcontinent are marked by large inequalities and little social protection [14], meaning that much of their

population is likely to be unable to absorb the shocks related to a changing environment. Moreover, the lack of sufficient and timely environmental monitoring on the ground is another issue. For instance, the World Air Quality Report 2022 [15] captures data from over 30 000 air quality monitoring stations, of which only 156 are located in Africa. Another study [16] highlights only 1 ground-level air quality monitor per 15.9 million people in sub-Saharan Africa. These conditions limit the power of national or international indicators to explain spatially varying environmental conditions. In light of these limitations, the role of publicly accessible spatial data on the environment is immense, allowing temporally and spatially efficient environmental monitoring and informing targeted adaptation strategies.

Environmental exposure studies [6, 8, 17–19] have demonstrated the wide applicability of remote sensing and geospatial data to link specific environmental indicators with demographic and health indicators. However, it is imperative to recognize that different environmental challenges often coexist in the same geographical location, compounding risks for the populations residing there [20].

In the context of this study, we focus on hazardous levels of $PM_{2.5}$, temperature increase, prolonged drought severity, and green deficit (scarcity of green trees) as key environmental risk factors, capturing climate and environmental change in their different dimensions. We report the simultaneous presence of more than one of these risk factors as 'multiple environmental burdens' (MEBs). We quantify the population exposed to each of these key environmental risk factors and to MEB in sub-Saharan Africa at the finest spatial resolution (1 km grid cell) for 2000 and 2019 and analyze the changes in exposure over this period. We also ask: What is the contribution of population change, environmental change, and their interaction to the change in exposure to specific environmental risk factors and MEB? The findings are then aggregated at national, regional, and subcontinental levels, providing a comprehensive understanding of the population exposed to environmental burdens in sub-Saharan Africa.

2. Data and methods

2.1. Data

Environmental burdens can be estimated on the basis of several indicators representing key environmental challenges. We have selected four major indicators measurable at a fine level, to partially account for global environmental challenges: air pollution (with $PM_{2.5}$), climate change (with temperature increase), extreme events (with prolonged severe drought), and land cover change (FCover vegetation index). To derive population and environmental indicators we employed publicly available raster data (geospatial pixelated data where each pixel presents the value of the defined indicator). The gridded population estimates are derived from the modeling of multiple spatial layers and population estimates from the census/surveys/United Nations' projected population [21]. All data were spatially processed (clipped, reprojected, rescaled, and aggregated using zonal statistics) using QGIS. The years 2000 and 2019 were selected to capture long-term changes and to avoid the temporary impact of COVID-19 restrictions on environmental parameters. Further, the selected years were also devoid of any major climate abnormalities associated with El Niño and La Niña occurrences. Such phases of abnormalities can deviate from the normal precipitation patterns and temperature levels, with which the studied risk factors are strongly associated.

Table 1 lists the details of the data used in this study.

2.2. Methods

2.2.1. Environmental burden and population exposure

We set thresholds to define the environmental risk factors as:

(a) Hazardous $PM_{2.5}$ levels: pixels with values above 20 μg m^{-3} (annual average). The air quality guidelines (AQGs) recommended by the World Health Organization [25] suggest that $PM_{2.5}$ above 5 μg m^{-3} is harmful, which is also referenced in many global studies dealing with their health impacts [2, 26]. Unsurprisingly, at this threshold, about 99% of the world's population is considered to be exposed to air pollution [27]. To detect extremely harmful levels of $PM_{2.5}$ and to relate the approach to globally accepted standards, we have chosen 20 μg m^{-3} as an appropriate threshold. Although four times higher than the AQG, this value falls between the WHO's second and third interim targets [25]. $PM_{2.5}$ is estimated by modeling aerosol optical depth estimates from various satellite instruments and then adjusting the retrievals to global ground-based observations of $PM_{2.5}$ using geographically weighted regression [22].

(b) Extreme temperature increase: pixels with a 1 °C increase or more, in average annual temperature compared to twenty years before (1980 is the reference year for 2000, and 2000 for 2019). This threshold represents about three times the global warming trend since 1981 (+0.18 °C per decade) [28]. Previous studies measured the number of days above certain temperature thresholds [29, 30] in order to capture heatwaves. In this study, we chose to capture the high-resolution change in average temperature over two decades that can account for the actual trends in temperature. In addition to the health impact, the average temperature increase can be linked to multiple aspects affecting the economy and sustainable development.

(c) Prolonged severe drought: pixels with PDSI $\leqslant -3$ for at least four months during the year and/or in

Table 1. Details of the data used in the study.

Indicator	Source	Spatial resolution and time
Population	WorldPop project [21]	∼1 km 2000, 2019
Fine particulate matter ($PM_{2.5}$)	Atmospheric Composition Analysis Group [22]	∼1 km 2000, 2019
Temperature	TerraClimate dataset [23], Climatology lab	∼4 km 1980, 2000, 2019
Palmer drought severity index (PDSI)		∼4 km 1999, 2000, 2018, 2019
Fraction of vegetation cover (FCover)	Copernicus Global Land Service [24]	∼1 km 1999, 2000, 2018, 2019

the previous year (1999–2000 are the reference years for 2000, and 2018–2019 for 2019). 24 months of data were used to reduce temporal irregularities. We avoided using annual averages of PDSI to detect drought duration and intensity, as annual measures can mask actual droughts. While there are other critically modeled indices of droughts [31], this index allows analyses at finer resolutions for the selected time period.

(d) Green deficit: pixels with an average FCover value of less than 0.3, that is, where less than 30% of the 1 km grid cell holds vegetation (tree canopy cover). This tree cover canopy represents the amount of greenery by trees (continuous/scattered) across forest/rural/urban lands. Here, we derived data on FCover for the same month (March) for each year to minimize seasonal variations in green canopy cover. Moreover, we averaged two years of data for each time period (average of 1999–2000 for 2000 and average of 2018–2019 for 2019) to avoid the impact of above-normal precipitation during any specific year that can increase the green canopy extent significantly.

Although a single risk factor at these thresholds may not pose a serious challenge to population exposure, the presence of MEBs at the same time and in the same place may cause serious detrimental impacts on the health and overall wellbeing of the exposed population. To estimate the coexistence of multiple risk factors, we have attempted to estimate MEB. To create raster layers of MEB, the four criteria-specific raster data were resampled and rescaled at ∼1 km resolution and superimposed. First, all four layers of risk factors were given binary values (0 and 1), where 1 represents the existence of a particular risk factor (pixel values above/below the set thresholds). Second, we added these four layers using the raster calculator to have a single-band raster with pixel values 0 (meaning absence of all risk factors) to 4 (meaning presence of all risk factors). Finally, we constructed three successive raster layers representing the presence of at least two (2EB), three (3EB), or four (4EB) of the abovementioned risk factors per pixel. To estimate the exposure, we multiply the population in each grid cell with each criteria-specific raster layer. We employed a similar approach as Jones *et al* [18] and subsequent exposure studies [27, 32–35]. The exposed population data were aggregated to country borders using zonal statistics.

2.2.2. Environmental and population effects on exposure

The change in population exposure to an environmental risk factor can be caused by population change, change in the area undergoing this environmental risk factor, or by the interaction of these two elements over time. Following previous studies [8, 18, 36], we decomposed the total change in exposure from 2000 to 2019 (ΔExp) into three components: the environmental effect, defined by the product of the population from base year and the change in the area under environmental risks ($P_{2000} \times \Delta Env$); the population effect, defined by the product of the population change from 2000 to 2019 and the area under extreme environmental conditions at base year ($\Delta P \times Env_{2000}$); and the interaction effect, that can be derived from the previous terms (by subtracting the sum of population and environmental effects from total exposure) but comes to the product of population change by the area under environmental change ($\Delta P \times \Delta Env$). The ΔExp is expressed as:

$$\Delta Exp = P_{2000} \times \Delta Env + \Delta P \times Env_{2000} + \Delta P \Delta Env \quad (1)$$

where: P_{2000} and ΔP are expressed in absolute numbers, ΔP being positive or negative; Env_{2000} is binary (0 when a pixel lies under the chosen threshold, 1 if it lies above) and ΔEnv takes the values -1, 0 or 1. The three effects are the results of the addition of positive and negative terms, the negative ones occurring for pixels where areas under environmental risk are improving ($\Delta Env = -1$) or where population is decreasing ($\Delta P \leqslant 0$). Globally, the interaction effect will be higher when there is simultaneous population growth and environmental degradation (as per our indicators) in one place, which is a common case but not the only scenario found in sub-Saharan Africa over the period 2000–2019, as we shall see in the results.

To obtain the percentage of each effect, we divided each effect by the total change in exposure ΔExp and multiplied by 100. A reduction in population or in the area under environmental risk results in negative terms in (1) and can lead to a decrease in exposure.

In addition to these, we have provided extended analysis in the supplementary material to indicate how a different set of thresholds (for two of the risk factors) can change the exposure estimates and spatial patterns of MEB. The extended analyzes also include results specific to four urban regions.

3. Results

3.1. Population exposure to hazardous $PM_{2.5}$ levels

Figure 1 illustrates population exposure to hazardous $PM_{2.5}$ levels in 2000 and 2020 (figures 1(a) and (b)) and country-level change, presented as absolute values in figure 1(c) and as percentages of the total population in supplementary table S1. The data reveal high $PM_{2.5}$ levels for both years as well as pronounced spatial disparities across countries that are not necessarily reflected in exposure since population distribution over the subcontinent is highly uneven and concentrated in a few regions. In sub-Saharan Africa, the population exposed to hazardous $PM_{2.5}$ levels rose from approximately 438 million (69%) in 2000 to about 898 million (80%) in 2019. At the regional level, West Africa exhibits markedly higher $PM_{2.5}$ concentrations, contrasting with Southern Africa, which experiences the lowest levels. The escalation is particularly significant in densely populated areas and regions experiencing notable population growth. Notably, it is the Central African region that exhibits the highest population exposure (98.5%).

At the country level, exposure to hazardous $PM_{2.5}$ levels has markedly increased in densely populated countries between 2000 and 2019. For instance, in Nigeria, the exposed population rose from approximately 115.65 million (99%) to about 206.59 million (99%), in the Democratic Republic of Congo from around 43.9 million (96%) to approximately 108.19 million (100%), and in Ethiopia from roughly 13.54 million (22%) to about 60.53 million (60%). Additionally, Eastern African countries such as Sudan, Uganda, Tanzania, and Kenya experienced a notable increase in exposure levels. In contrast, marginal reductions in exposure were observed in Eswatini, Namibia, and Botswana. However, South Africa, despite its proximity to these three countries, witnessed a significant increase in exposure, rising from approximately 24 million to about 35 million.

3.2. Population exposure to extreme temperature increase

The spatial patterns of temperature increase across sub-Saharan Africa and populated areas are presented in figures 2(a) and (b) for 2000 and 2019, respectively. The temperature increase is measured relatively to levels from two decades prior (1980–2000 for 2000, 2000–2019 for 2019). The visual representations clearly indicate a high temperature increase across most of the subcontinent. Interestingly, while temperature rise was not a significant concern in 2000, it became prevalent over the subsequent decades. However, in 2019, population concentrations were primarily situated in areas where temperature increase was not extreme (figure 2(b)).

Our analysis focuses on populations residing in areas with extreme temperature increase (exceeding 1 °C). Figure 2(c) provides country-level aggregated statistics of the exposed population for 2000 and 2019, displayed in absolute values, while percentages of the total population are presented in supplementary table S1. In sub-Saharan Africa, the population exposed to extreme temperature increase rose from approximately 30 000 (0.01%) in 2000 to around 16 million (1.4%) in 2019. At the regional level, Southern Africa accounted for the largest share of the exposed population (2.6%) compared to other regions. A noticeable heterogeneity in exposure levels is evident at the country level. Remarkably, in 2019, countries with relatively high population exposure included Ethiopia (∼2.24 million), DR Congo (∼1.93 million), South Africa (∼1.74 million), and Angola (∼1.15 million), among others. The significantly lower change in exposure in Nigeria embodies the little influence of population size or growth on the levels of exposure. Some countries, such as Guinea-Bissau, Gambia, and Burundi had close to zero exposure to extreme temperature increase in 2019.

3.3. Population exposure to prolonged severe drought

Figures 3(a) and (b) illustrate the spatial patterns of the Palmer drought severity index (PDSI) alongside population concentrations in 2000 and 2019, respectively. According to our definition, prolonged severe drought conditions correspond to areas experiencing PDSI $\leqslant -3$ for at least four months during the year and/or previous year. Country-level estimates for 2000 and 2019 are depicted in figure 3(c) (absolute values) and supplementary table S1 (percentages).

An evident escalation in areas facing drought severity is observable across the subcontinent from 2000 to 2019. The population exposed to prolonged severe drought has increased substantially, rising from approximately 9.35 million (1.5%) in 2000 to about 22.68 million (2%) in 2019 (figure 3(c), table S1). East Africa exhibits a relatively higher share of population exposure, accounting for 2% in 2000 and 2.5% in 2019, in comparison to other regions.

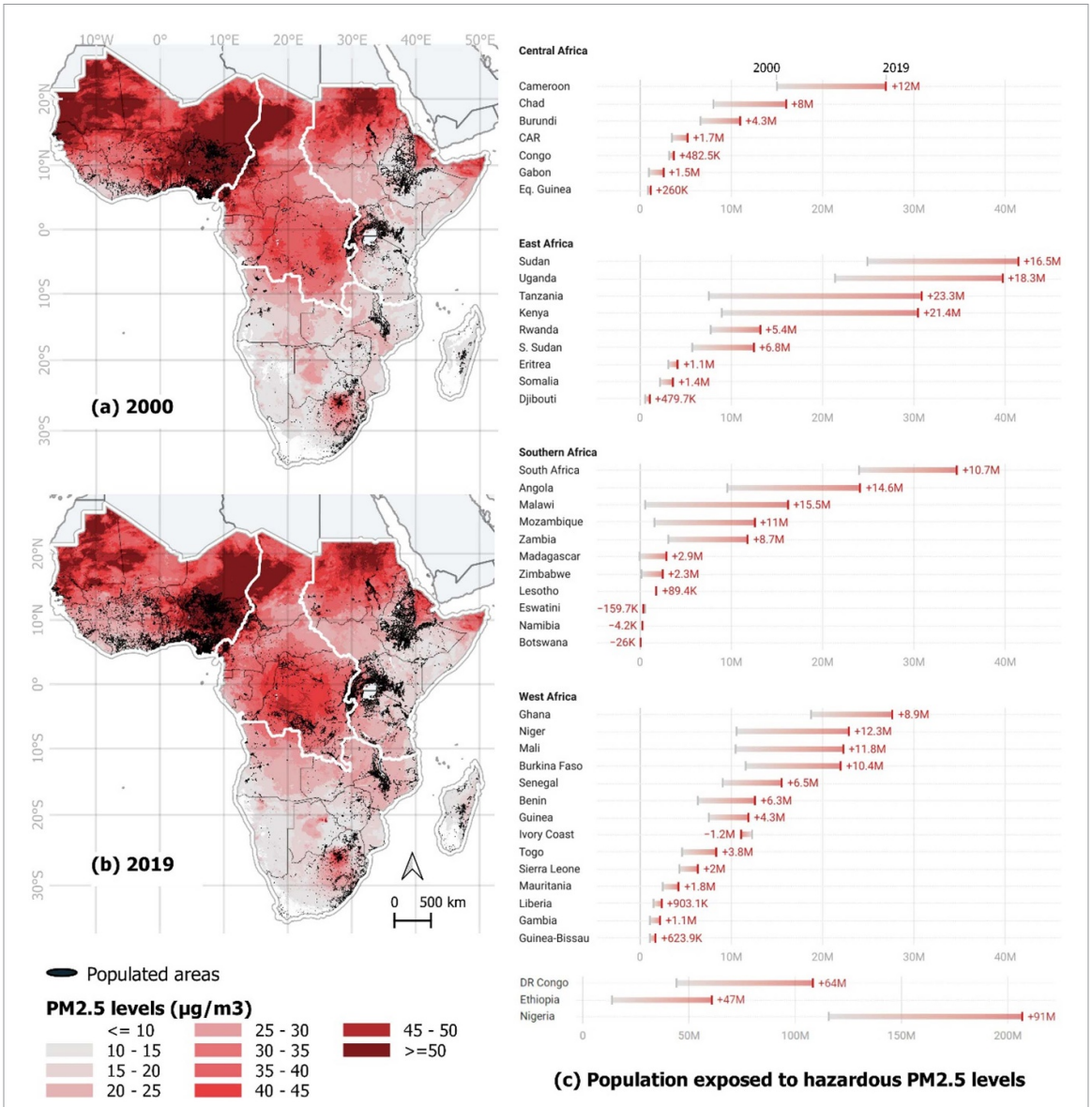

Figure 1. $PM_{2.5}$ concentrations and population exposure. (a) Spatial patterns of $PM_{2.5}$ (from grey to red) and populated areas (pixels with more than 100 persons) in 2000 (black); (b) spatial patterns of $PM_{2.5}$ and populated areas (pixels with more than 100 persons) in 2019; (c) country-wide levels of population exposed to hazardous $PM_{2.5}$ (>20 μg m3). The three most populated countries—DR Congo (Central Africa), Ethiopia (East Africa), and Nigeria (West Africa)—are presented on a separate scale.

However, a closer country-level examination reveals significant disparities in exposure and exposure change. In 2019, countries with high population exposure included highly populated nations such as DR Congo (∼3.6 million or 3.3%), Ethiopia (∼2.3 million or 2.3%), Kenya (∼1.8 million or 3.5%), South Africa (∼1.7 million or 2.9%), and Nigeria (1.2 million or 0.6%). Notably, the changes in exposure also differ among these countries. For instance, South Africa experienced a substantial increase in exposure (1.6 million), whereas Nigeria witnessed only a marginal rise (48 000) from 2000 to 2019. Conversely, other countries experienced a decline in exposure over this period: Madagascar (−371 000), Sierra Leone (−90 000), and Zambia (−80 000). These varied exposure and changes seem to stem from both the varying severity of drought over space and time and population growth in affected areas.

3.4. Population exposure to green deficit

FCover indicates the fraction of green vegetation cover in a unit area, based on a two-year average of measures taken in the month of March, and ranges from 0 to 1. We considered green deficit as FCover values lower than 0.3. This threshold signifies areas with very limited green tree cover, which can potentially add to challenges like urban heat islands and also highlight the areas where better land-use planning is needed.

As illustrated in figures 4(a) and (b), the greener areas are concentrated mainly over the central parts

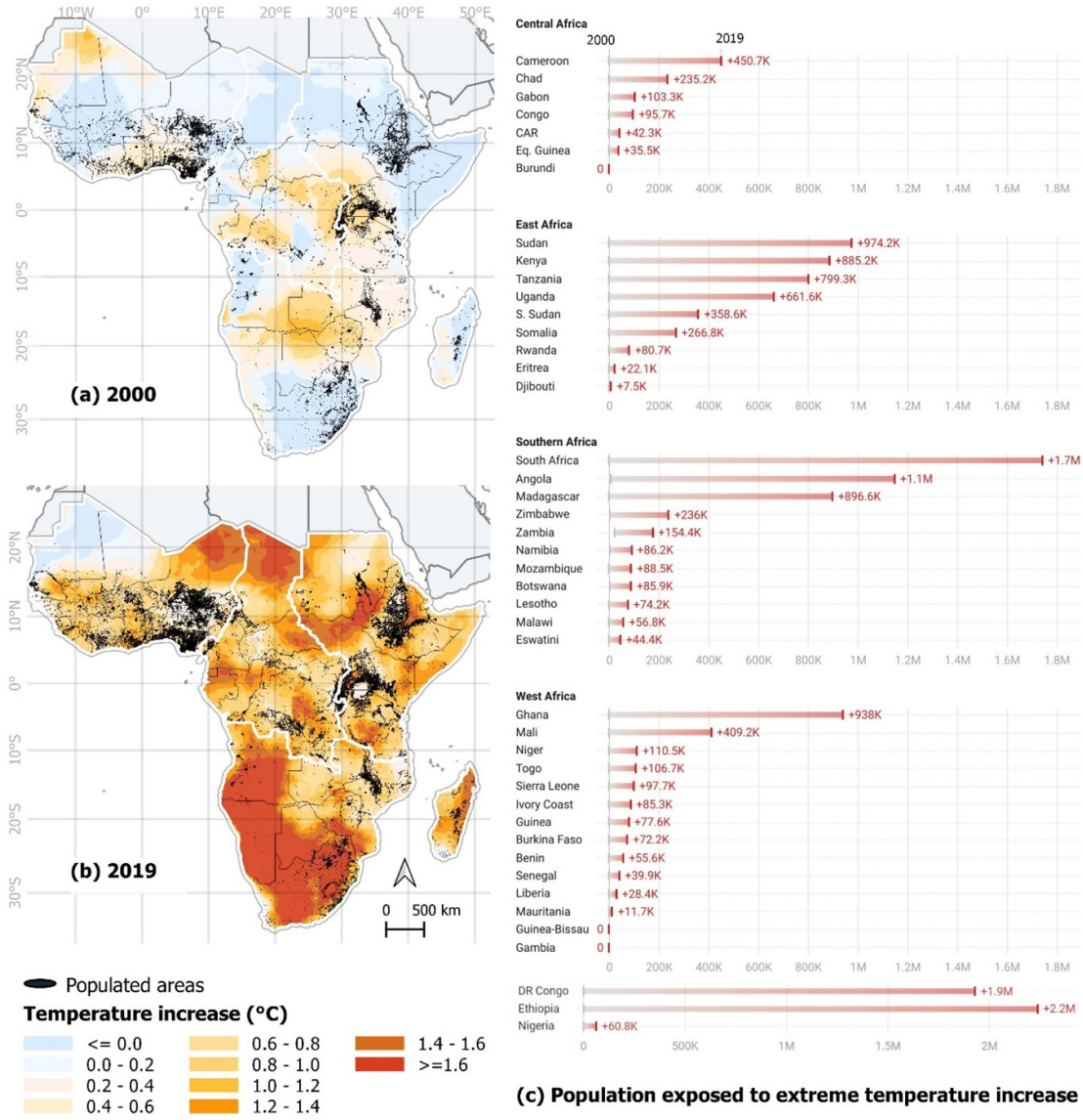

Figure 2. Temperature increase and population exposure. (a) Spatial patterns of temperature increase (sky blue to orange) and populated areas (pixels with more than 100 persons) in 2000 (black); (b) spatial patterns of temperature increase and populated areas (pixels with more than 100 persons) in 2019; (c) country-wise levels of population exposed to extreme temperature increase (>1 °C increase in average annual temperature compared to the reference year -twenty years- before). The three most populated countries—DR Congo (Central Africa), Ethiopia (East Africa), and Nigeria (West Africa)—are presented on a separate scale.

of the subcontinent in both years. Overall FCover levels in sub-Saharan Africa have remained largely stable, especially in unpopulated regions. However, a contrasting trend is observed over populated areas, where serious challenges are evident. The population exposed to green deficit has more than doubled over 20 years, increasing from approximately 291 million (45.6%) in 2000 to approximately 537 million (48%) in 2019 (table S1). Regionally, West and East Africa bear the highest population exposure, accounting for 68.3% and 62.4% in 2019, respectively.

Country-level exposure and its changes are detailed in figure 4(c) (absolute values) and supplementary table S1 (percentages). Highly populated countries exhibited significantly high exposure levels and notable changes over time, including Nigeria, from ∼71 million (61%) to ∼140 million (67%), Ethiopia, from ∼53 million (87%) to ∼72 million (71%), Sudan, from ∼25 million (99%) to ∼40 million (97%), Kenya, from ∼15 million (52%) to ∼23 million (45%), and Niger, from ∼11 million (100%) to ∼23 million (100%). Rapid increases in both the absolute and percentage of the population exposed were observed in several countries, such as South Africa, Angola, and Ghana. Remarkably, despite higher exposure levels in 2019, the percentage of the population exposed to green deficit decreased in many countries. A negative change in exposure was observed only in Lesotho, where the population remained stable from 2000–2019, contributing to an improvement in FCover values.

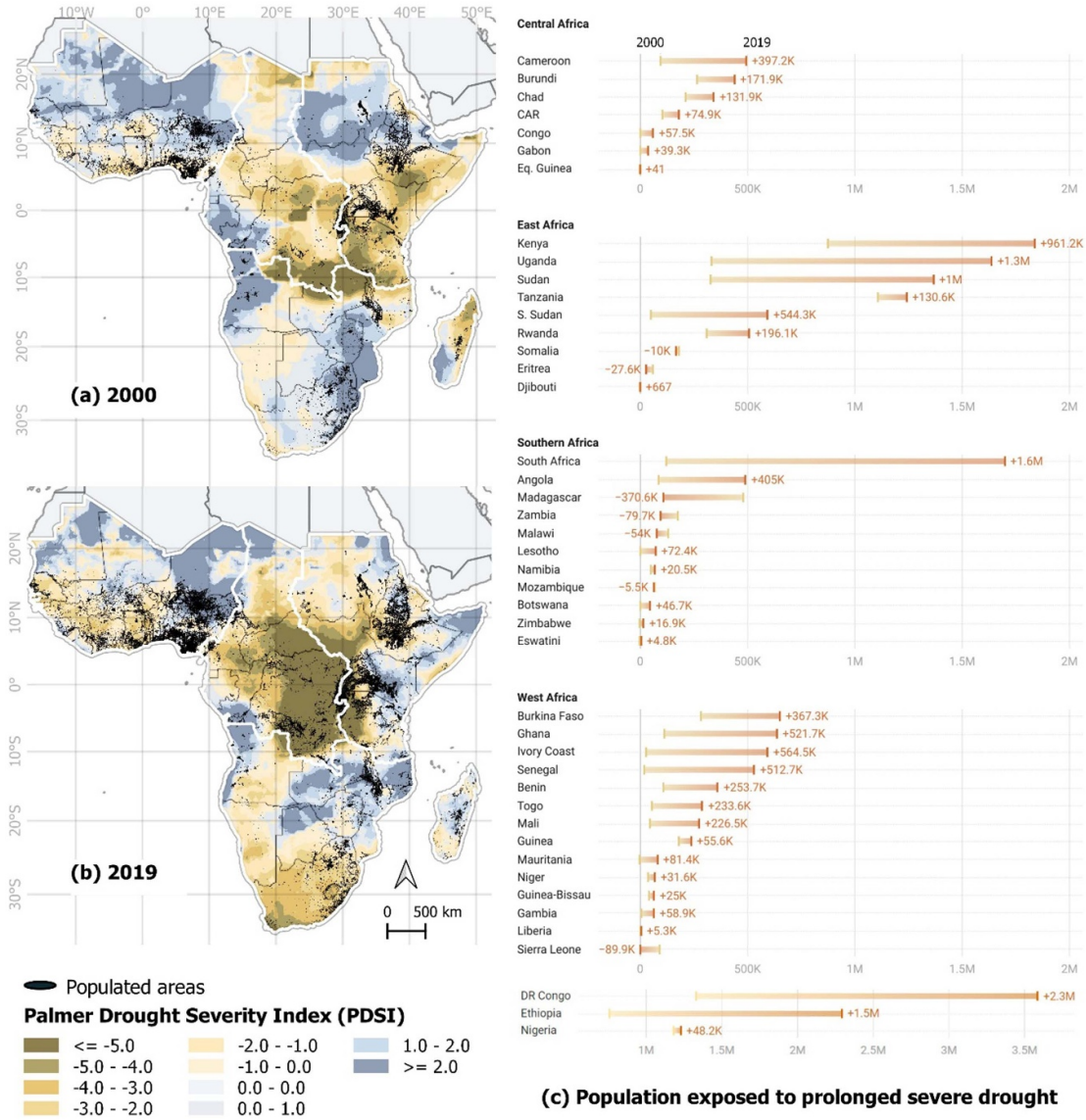

Figure 3. Drought severity and population exposure. (a) Spatial patterns of average PDSI of 24 months-1999 & 2000 (tan to slate grey) and populated areas (pixels with more than 100 persons) in 2000 (black); (b) spatial patterns of PDSI (average of 24 months—2018 & 2019) and populated areas (pixels with more than 100 persons) in 2019; (c) country-wise levels of population exposure to prolonged severe drought (PDSI $\leqslant -3$ for at least four months during the year and/or in the previous year). The three most populated countries—DR Congo (Central Africa), Ethiopia (East Africa), and Nigeria (West Africa)—are presented on a separate scale.

3.5. Population exposure to MEBs

Figures 5(a) and (b) illustrate the spatial distribution of MEBs, alongside populated areas for 2000 and 2019, respectively. The analysis identifies areas characterized by at least two (2EB), three (3EB), or four (4EB) environmental risk factors. A noticeable expansion in the regions concerned by MEB is evident over time. In 2000, the majority of the subcontinental area exhibited 2EB. However, by 2019, there was a significant increase in areas with 3EB, and patches characterized by all four risk factors (4EB) became apparent. Figure S2 illustrates the spatial patterns of change in MEB over the past twenty years. Although, positive change dominates the regions, there are areas with no and negative change in the MEB (figure S2).

We reported exposure by identifying the number of people living in each grid cell with MEBs (2EB, 3EB, and EB) for both years. Table 2 shows total and country-level exposure numbers.

At the subcontinental level, the population exposed to MEB experienced a remarkable increase over the study period. Specifically, there was an increase in population exposure from approximately 300 million to about 465 million for 2EB, from around 47 million to approximately 292 million for 3EB, and from none to approximately 92 million for 4EB. In 2019, several East African countries witnessed substantial population exposure to 4EB, including Sudan (∼22.3 million), Ethiopia (∼18 million), South Sudan (∼7.6 million), and

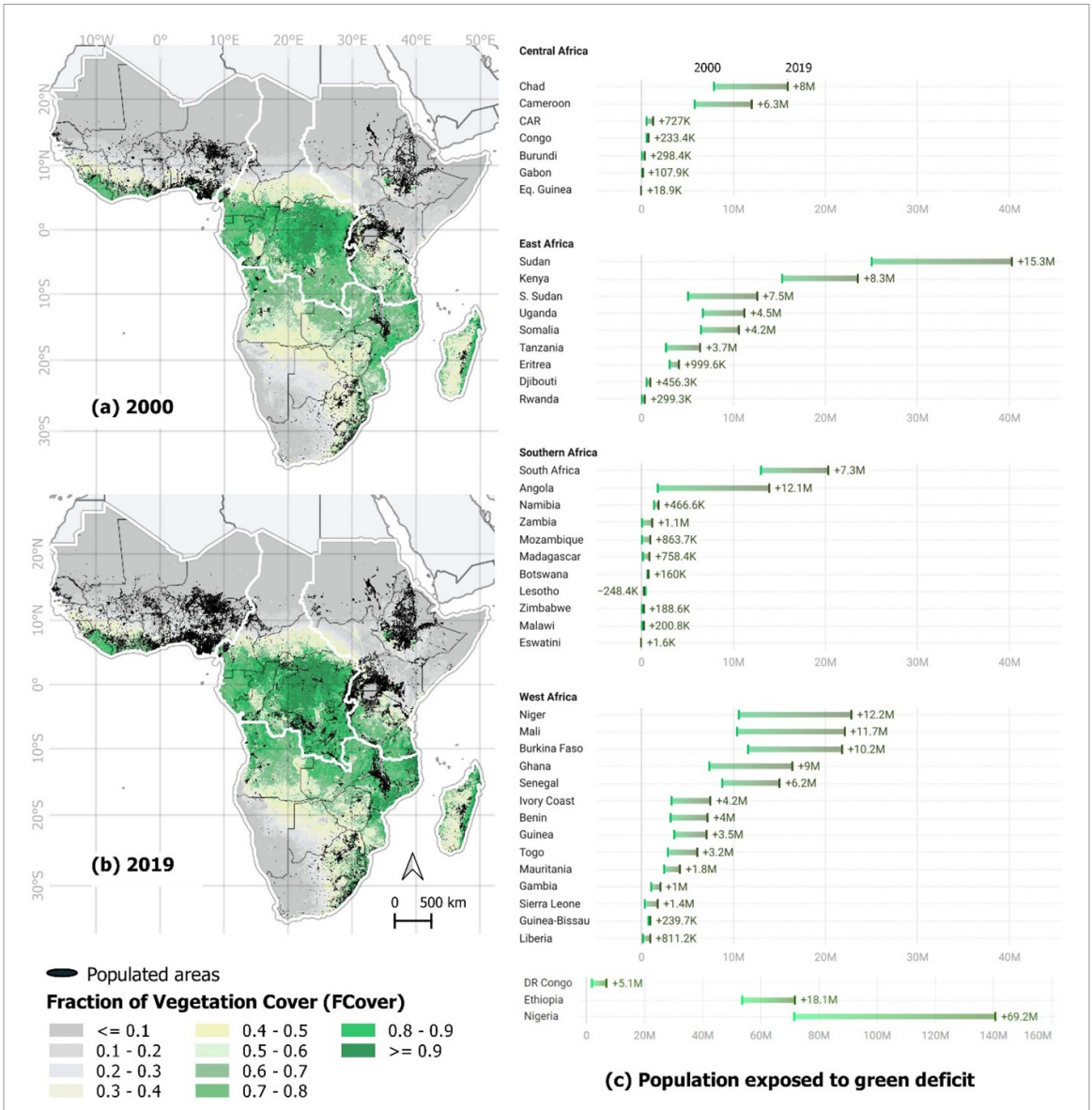

Figure 4. Green deficit and population exposure. (a) Spatial patterns of average FCover of 1999 & 2000 (grey to green) and populated areas (pixels with more than 100 persons) in 2000 (black); (b) spatial patterns of FCover (average of 1999 & 2000) and populated areas (pixels with more than 100 persons) in 2019; (c) country-wise levels of population exposure to green deficit (FCover < 0.3 for average of the last two years). The three most populated countries—DR Congo (Central Africa), Ethiopia (East Africa), and Nigeria (West Africa)—are presented on a separate scale.

Kenya (∼5.4 million). Other countries with higher levels of population exposed to 4EB included South Africa (∼8.3 million), and Ghana (∼5.5 million). The population exposed to 2EB or 3EB increased in most countries in sub-Saharan Africa. Notable increases in population exposure to 3EB were observed in specific countries, such as DR Congo (from 0.6 to 44.2 million), Ethiopia (from 1.2 to 22.7 million), Uganda (from 1.8 to 21.2 million), South Africa (from 0 to 19.7 million), Kenya (from 1 to 17.6 million), and Ghana (from 0.5 to 13.4 million), among others.

3.6. Environmental and population effects on exposure

To elucidate the factors driving change in exposure to different environmental risk factors from 2000 to 2019, we have distinguished the components of this exposure change (environmental effect, population effect, and interaction effects) for sub-Saharan Africa (figure 6).

About 460 million more people are exposed to hazardous $PM_{2.5}$ levels in 2019. The population effect accounts for the major part of this change in exposure, contributing 81% (∼373 million) of the total (figure 6(a)), whereas the environmental effect constitutes only 11% (∼50 million) and the interaction effects only 8% (∼37 million) of the total. This underscores the pivotal role of the significant population increase, primarily in areas where $PM_{2.5}$ levels have consistently exceeded the threshold over time.

About 16 million more people are exposed to extreme temperature increase. The population effect

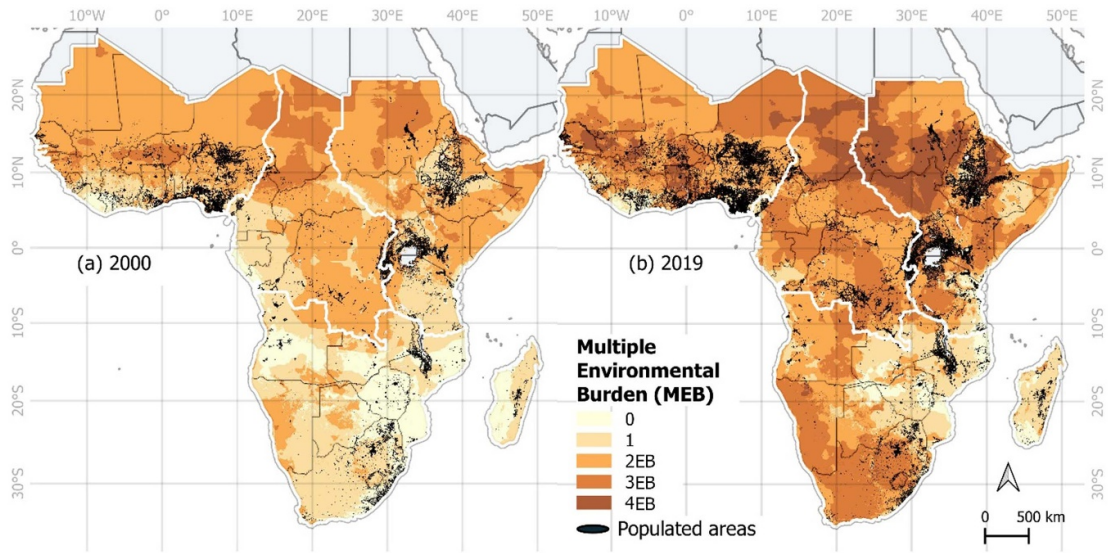

Figure 5. Multiple environmental burdens (MEB) and population exposure. (a) Spatial patterns of MEB (light to dark blue) and populated areas (pixels with more than 100 persons) in 2000 (black); (b) spatial patterns of MEB and populated areas (pixels with more than 100 persons) in 2019.

constitutes only 1% (0.1 million) of the total change. Here, the change in exposure is predominantly influenced by the environmental effect, contributing to 57% (∼9 million) of the total, and the interaction effect accounting for 43% (∼7 million) of the total change (figure 6(b)). This pattern underscores the critical role played by the expansion of areas with extreme temperature increases and the synergistic interactions between these areas and the changing population in driving the surge in exposure.

In the change in exposure to prolonged severe drought (∼13 million), all three components play significant roles, with the population effect contributing 53% (∼7 million) of the total, while the environmental and interaction effects account for 27% (∼3.6 million) and 20% (∼2.7 million) of the total, respectively (figure 6(c)). This distribution highlights the dynamic interplay between changes in population and areas facing severe drought, driving enhanced exposure over time.

In the context of the change in exposure to green deficit (∼246 million), the population effect significantly dominates, contributing 105% (∼258 million) to the total change. This is partially countered by the environmental effect (−3% or ∼ −7 million) and interaction effect (−2% or ∼ −5 million) to the total change in exposure (figure 6(d)). These results shed light on a situation where population increase is notably high in areas characterized by green deficit. Additionally, it suggests slight improvements in green cover from 2000 to 2019, indicated by negative values for both environmental and interaction effects.

To analyze the change in population exposure to MEBs, we reported changes in exposure to at least three risk factors (3EB) and their contributing factors (figure 6(e) for sub-Saharan Africa and supplementary figure S1 for country-specific effects). The total change in exposure to 3EB (∼246 million) attributed to the environmental effect constitutes 48% (∼119 million) of the total, whereas the change caused by interaction effects accounts for 36% (∼89 million) of the total. In contrast, the population effect contributes only 15% (∼37.6 million) of the total. This underscores the remarkable expansion of areas with 3EB, coinciding with a simultaneous increase in population over time. Similar patterns of change in exposure to 3EB were observed in the majority of the countries, where environmental effects played a more significant role in driving country-specific changes in exposure (figure S1).

4. Discussion

We investigated population exposure to environmental risk factors—hazardous $PM_{2.5}$ levels, extreme temperature increases, prolonged severe drought, green deficit—and MEBs across sub-Saharan Africa from 2000 to 2019. Our results indicate a significant escalation in specific environmental risk factors and MEB, which, in conjunction with population growth, leads to an increasing population exposure.

The extreme levels and increases in $PM_{2.5}$ concentrations have been the highlights of previous studies [37–39]. Multiple sources of $PM_{2.5}$ can be identified. Dust from the Sahara desert contributes to higher concentrations of $PM_{2.5}$ in parts of western sub-Saharan Africa, while fossil fuel use (coal, liquid oil, and natural gas) is a major contributor in southern Africa [26]. The observed spatial patterns highlight a stark contrast in $PM_{2.5}$ concentrations

Table 2. Country-level population exposure to multiple environmental burdens in 2000 and 2019.

	Year 2000—population exposed to					Year 2019—population exposed to					
	2EB		3EB			2EB		3EB		4EB	
	Millions	%	Millions	%	4EB	Millions	%	Millions	%	Millions	%
Central Africa	**50**	58.3	**8**	9.3	**0**	**88**	50.2	**65**	37.1	**7**	4.0
Burundi	6.6	98.7	0	0.0	0	10.6	95.9	0.4	3.6	0	0.0
Cameroon	4.6	30.6	1.8	12.0	0	8.3	30.6	9.1	33.6	3	11.1
CAR	2.6	72.8	0.4	11.2	0	3	57.4	2.1	40.1	0.1	1.9
Chad	2.8	34.9	5.2	64.8	0	5.6	35.0	6.2	38.8	4.1	25.6
Congo	0.5	11.0	0	0.0	0	0.9	24.0	1.9	50.6	0	0.0
DR Congo	32.4	70.9	0.6	1.3	0	57.1	52.7	44.2	40.8	0.1	0.1
Eq. Guinea	0	0.0	0	0.0	0	0.9	74.5	0	0.0	0	0.0
Gabon	0	0.0	0	0.0	0	1.5	53.2	0.9	31.9	0	0.0
East Africa	**93.2**	**47.6**	**15.6**	**8.0**	**0**	**131.9**	**39.3**	**96.2**	**28.6**	**57**	**17.0**
Djibouti	0.5	85.4	0	0.0	0	0.8	75.1	0.2	18.8	0	0.0
Eritrea	1.7	53.4	1.4	44.0	0	3.3	78.8	0.3	7.2	0.5	11.9
Ethiopia	23.5	38.3	1.2	2.0	0	45.2	44.7	22.7	22.5	18	17.8
Kenya	15.6	53.3	1	3.4	0	19.9	37.7	17.6	33.4	5.4	10.2
Rwanda	7.6	97.3	0.1	1.3	0	10.7	81.0	2.4	18.2	0	0.0
S. Sudan	4.5	74.1	0.8	13.2	0	3.6	23.2	3.5	22.6	7.6	49.1
Somalia	4.9	74.0	0.7	10.6	0	5.5	50.2	4.3	39.2	0	0.0
Sudan	16.6	66.0	8.1	32.2	0	6.7	16.1	11.9	28.7	22.6	54.5
Tanzania	8.6	26.4	0.4	1.2	0	19.1	35.0	12.1	22.2	0.3	0.5
Uganda	9.7	41.9	1.8	7.8	0	17.1	41.6	21.2	51.6	2.5	6.1
Southern Africa	**13.9**	**10.4**	**0.2**	**0.1**	**0**	**48.2**	**23.4**	**31.8**	**15.4**	**13.1**	**6.4**
Angola	2.1	10.4	0	0.0	0	14.9	44.8	7.6	22.8	4.4	13.2
Botswana	0.1	6.1	0	0.0	0	1	42.7	0.5	21.3	0	0.0
Eswatini	0	0.0	0	0.0	0	0.5	46.3	0	0.0	0	0.0
Lesotho	0.4	21.5	0	0.0	0	0	0.0	1.6	85.8	0.3	16.1
Madagascar	0.1	0.7	0	0.0	0	4.3	16.1	0.4	1.5	0	0.0
Malawi	0.1	0.9	0	0.0	0	2.4	13.3	0.1	0.6	0	0.0
Mozambique	0	0.0	0	0.0	0	1.7	5.7	0	0.0	0	0.0
Namibia	0.9	49.0	0.1	5.4	0	0.7	29.0	1.3	53.9	0.1	4.1
South Africa	7.9	17.9	0	0.0	0	17.8	30.3	19.7	33.5	8.3	14.1
Zambia	2.4	24.9	0	0.0	0	4	22.4	0.5	2.8	0	0.0
Zimbabwe	0	0.0	0	0.0	0	0.9	6.4	0	0.0	0	0.0
West Africa	**142.4**	**63.8**	**22.9**	**10.3**	**0**	**197.5**	**49.3**	**99.8**	**24.9**	**14.4**	**3.6**
Benin	3.6	56.4	1	15.7	0	6.4	50.7	5.2	41.2	0.3	2.4
Burkina Faso	4.5	38.7	7.1	61.1	0	5	22.7	15.7	71.4	1.1	5.0
Gambia	0.8	68.1	0.1	8.5	0	0.5	22.1	1.6	70.8	0	0.0
Ghana	8.9	47.3	0.5	2.7	0	8.5	26.7	13.4	42.1	5.5	17.3
Guinea	3.8	49.2	1.9	24.6	0	5.4	45.1	4.1	34.2	0.4	3.3
Guinea-Bissau	0.5	43.9	0.6	52.7	0	0.8	45.3	0.9	51.0	0	0.0
Ivory Coast	2.8	17.9	0.3	1.9	0	8.2	32.4	3.2	12.7	0	0.0
Liberia	0.2	7.2	0	0.0	0	1	23.7	0.1	2.4	0	0.0
Mali	9.2	88.1	1.2	11.5	0	8.3	37.3	10.4	46.7	3.4	15.3
Mauritania	2.4	96.3	0	0.0	0	2.2	51.3	1.7	39.7	0.3	7.0
Niger	9.6	90.5	1	9.4	0	18.3	80.0	4.5	19.7	0	0.0
Nigeria	83.4	71.8	8	6.9	0	125.6	60.2	22	10.5	0.9	0.4
Senegal	7.8	85.2	0.4	4.4	0	1.8	11.4	11.9	75.4	0.9	5.7
Sierra Leone	1.6	36.2	0.4	9.0	0	3.2	49.8	0.5	7.8	0	0.0
Togo	3.4	73.6	0.4	8.7	0	2.2	26.1	4.5	53.5	1.5	17.8
Sub-Saharan Africa	**299.1**	**46.9**	**46.6**	**7.3**	**0**	**465.5**	**41.6**	**292.5**	**26.2**	**91.8**	**8.2**

across different regions. This spatial heterogeneity in air pollution is contributed from the complex interplay of environmental factors [40, 41], population density [42], and urbanization [9]. Our analyses found a prominent role of population increase in the unprecedented surge in population exposure to extreme $PM_{2.5}$ levels (∼460 million). South Africa, despite being geographically close to countries with exceptionally lower exposure (Eswatini, Namibia, and Botswana), experienced a notable increase in exposure levels. This spatial variation within neighboring countries emphasizes the localized nature of air pollution sources (particularly transport emissions) [43], especially in the most urbanized countries [26].

The steep rise in temperatures over the past 20 years has highlighted the challenges of global

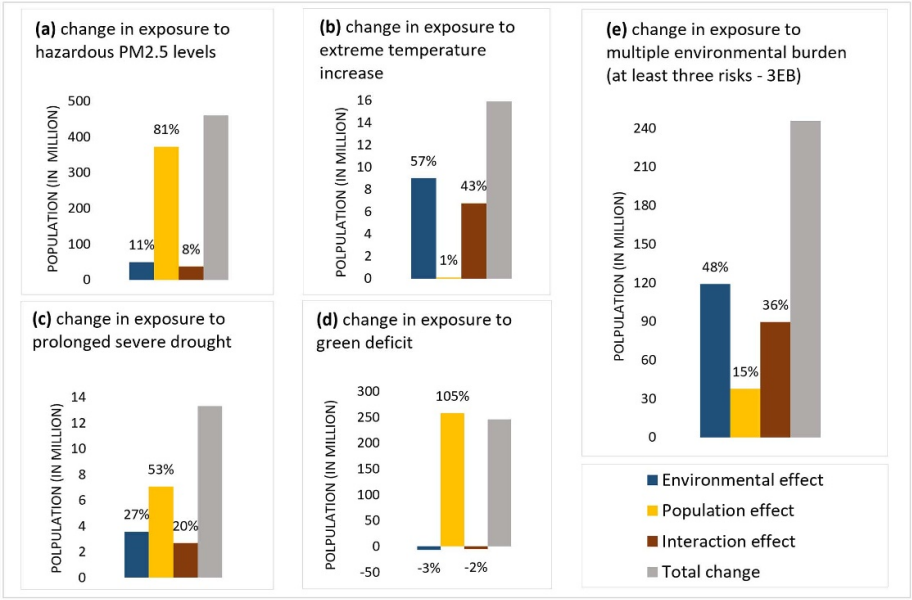

Figure 6. Contribution of environmental effect, population effect, and interaction effect in the change in population exposure from 2000 to 2019 to (a) hazardous $PM_{2.5}$ levels, (b) extreme temperature increase, (c) prolonged drought severity, (d) green deficit, and (e) multiple environmental burdens (at least three risks—3EB).

warming and climate change on the subcontinent. These conditions present severe challenges to public health [6, 7], socioeconomic stability [44] agriculture [45, 46], and the overall development of a region. We find an alarming increase in population exposure (from 30 000 to 16 million), emphasizing the growing exposure of populations to climate change in the form of increasing temperature. Exposure at the national level indicates regional disparities in the impact of rising temperatures on populations. Interestingly, the study identifies Nigeria as an exception, with a significantly lower change in exposure despite its large population. At the subcontinental level, the change in exposure is largely driven by the expansion of areas with extreme temperature increase and by the interaction effect rather than by population growth itself.

The increased exposure to prolonged severe drought highlights a growing vulnerability of communities to water scarcity and agricultural challenges [47–49]. Interestingly, the changes in exposure over time vary significantly among countries. For instance, South Africa saw the highest increase in exposure, with approximately 1.6 million more people exposed to prolonged severe drought in 2019. In contrast, Nigeria experienced a marginal increase in exposure, emphasizing the complex interplay of factors influencing vulnerability, including population size and varying drought severity over space and time. At subcontinental levels, the change in exposure to prolonged severe drought is contributed by all three factors, i.e. change in population, change in the areas under prolonged drought, and interaction between these two.

The greening of African drylands has already been reported [50]. A recent study by Wei *et al* [51]. Reports gains in woodland forests, rainforests, and savannas from 2000 to 2020, with spatially varying patterns. However, as little population is located in these areas, our results show an alarming increase in population exposure to green deficit (∼246 million) underscoring growing land use challenges [52]. Higher exposure to green deficit is also a characteristic of high population density in the urban regions that are devoid of green spaces, and are at higher subsequent risks such as heat exposure [53], air pollution [54], and associated health problems [55]. Highly populated countries experienced increasing exposure to green deficit. Population increase substantially offsets greening effects and drives an increase in exposure to green deficit over time. Despite the high levels of exposure to green deficit in 2019, it is noteworthy that the share of the population exposed to green deficit has declined in some countries. This decline could be attributed to various factors, including potential afforestation efforts, reforestation projects, or natural regrowth of vegetation [50].

Our findings showcase a substantial increase in MEB and exposed population. In 2019, specific countries in East Africa (Sudan, Ethiopia, South Sudan, and Kenya) experienced significant exposure to 4EB. Other countries, including South Africa and Ghana, also reported high levels of exposure to 4EB, highlighting the widespread nature of this issue. The DR Congo experienced a remarkable escalation in population exposure to 3EB, from 0.6 million to 44.2 million (followed by Ethiopia, Uganda, South Africa, Kenya, and Ghana). The increase in exposure to 3EB

is mainly due to environmental change and its interaction with population change.

5. Conclusion

Our results emphasize the urgency of addressing the challenges of increasing population exposure to environmental risk factors for the well-being of the population and the sustainability of the environment. Given the spatially heterogeneous patterns of population exposure, there is a strong need for targeted regional interventions, keeping in focus the relative roles of population and environmental factors in driving exposure change. There is an urgent need for air pollution and climate change mitigation [56, 57] in sub-Saharan Africa. This situation demands strategies to face the health risks associated with prolonged exposure to high $PM_{2.5}$ levels [58] as well as to enhance water resource management, promote sustainable agricultural practices, and improve community resilience to heat and drought-related challenges.

Our study is a pioneering effort in understanding MEB dynamics in sub-Saharan Africa from 2000 to 2019. The critically defined thresholds made it possible to identify populated areas with extreme environmental risks and MEB as per our objectives. Our approach, at a 1 km grid cell, offers crucial information for policy formulation and targeted interventions at national, regional, and subcontinental levels, with the possibility of defining different thresholds.

However, our study has limitations. Social and demographic indicators were limited, hindering our understanding of population vulnerability and adaptive capacity. We did not fully account for extreme events, which can impact environmental parameters [48, 59] and exposure levels. Defining environmental burdens solely based on four parameters is restrictive. There is a need to incorporate more environmental factors into MEB analysis.

Integrating social and demographic indicators into future studies would provide a holistic understanding of the interplay between environmental challenges and human societies. Exploring the links between MEB and public health outcomes could deepen our understanding of long-term environmental exposure effects on human well-being. Since environmental indicators have different levels and severity in urban and rural places, future studies can distinguish exposure between them. Additionally, including more parameters and conducting region-specific analyses could offer valuable insights into localized environmental challenges, aiding in the development of targeted mitigation strategies.

Data availability statement

The gridded population data are retrievable from the Worldpop project (www.worldpop.org/). The raster data of $PM_{2.5}$ can be downloaded from the Atmospheric Composition Analysis Group (https://sites.wustl.edu/acag/). The estimated values of temperature and PDSI are derivable from the Climatology Lab (www.climatologylab.org/). The FCover data can be accessed from the Copernicus Global Land Service (https://land.copernicus.eu/).

All data that support the findings of this study are included within the article (and any supplementary files).

Acknowledgments

This work is supported from the funding received as a post-doctoral contract of the first author with the Laboratoire d'excellence (Labex) iPOPs project hosted at the Institut national d'études démographiques (Ined), France. We thank all the open-access data providers (as described in the data availability statement).

Conflict of interest

The authors declare no conflicts of interest relevant to this study.

Author contribution

A S: Conceptualization, Data Curation, Formal Analysis, Methodology, Project administration, Visualization, Writing-original draft, Writing-review & editing; **V G:** Methodology, Project administration, Supervision, Writing-review & editing.

ORCID iD

Ankit Sikarwar https://orcid.org/0000-0001-9014-5921

References

[1] Calvin K *et al* 2023 Climate change 2023: synthesis report. Contribution of working groups I, II and III to the sixth assessment report of the intergovernmental panel on climate change ed H Lee and J Romero (Core Writing Team) (IPCC) (available at: www.ipcc.ch/report/ar6/syr/)

[2] Shaddick G, Thomas M L, Mudu P, Ruggeri G and Gumy S 2020 Half the world's population are exposed to increasing air pollution *npj Clim. Atmos. Sci.* **3** 1–5

[3] UNEP & FAO 2020 The state of the World's forests: forests, biodiversity and people (UNEP—UN Environment Programme) (available at: www.unep.org/resources/state-worlds-forests-forests-biodiversity-and-people)

[4] World Health Organization 2018 Preventing disease through healthy environments: a global assessment of the burden of disease from environmental risks (available at: www.who.int/publications-detail-redirect/9789241565196)

[5] Busby J W, Smith T G and Krishnan N 2014 Climate security vulnerability in Africa mapping 3.01 *Political Geogr.* **43** 51–67

[6] Baker R E and Anttila-Hughes J 2020 Characterizing the contribution of high temperatures to child undernourishment in Sub-Saharan Africa *Sci. Rep.* **10** 18796

[7] Amegah A K, Rezza G and Jaakkola J J 2016 Temperature-related morbidity and mortality in

Sub-Saharan Africa: a systematic review of the empirical evidence *Environ. Int.* **91** 133–49
[8] Iyakaremye V, Zeng G, Yang X, Zhang G, Ullah I, Gahigi A, Vuguziga F, Asfaw T G and Ayugi B 2021 Increased high-temperature extremes and associated population exposure in Africa by the mid-21st century *Sci. Total Environ.* **790** 148162
[9] Wei G, Sun P, Jiang S, Shen Y, Liu B, Zhang Z and Ouyang X 2021 The driving influence of multi-dimensional urbanization on $PM_{2.5}$ concentrations in Africa: new evidence from multi-source remote sensing data, 2000–2018 *Int. J. Environ. Res. Public Health* **18** 9389
[10] Verschuren D, Laird K R and Cumming B F 2000 Rainfall and drought in equatorial east Africa during the past 1,100 years *Nature* **403** 410–4
[11] Lamb P J 1982 Persistence of Subsaharan drought *Nature* **299** 46–48
[12] Reij C P and Smaling E 2008 Analyzing successes in agriculture and land management in Sub-Saharan Africa: is macro-level gloom obscuring positive micro-level change? *Land Use Policy* **25** 410–20
[13] World Bank 2020 The number of poor people continues to rise in Sub-Saharan Africa, despite a slow decline in the poverty rate (available at: https://blogs.worldbank.org/opendata/number-poor-people-continues-rise-sub-saharan-africa-despite-slow-decline-poverty-rate)
[14] Fosu A K 2015 Growth, inequality and poverty in Sub-Saharan Africa: recent progress in a global context *Oxf. Dev. Stud.* **43** 44–59
[15] IQAir 2022 IQAir | first in air quality *World Air Quality Report—2022* available at: www.iqair.com/world-air-quality-report
[16] Pinder R W, Klopp J M, Kleiman G, Hagler G S W, Awe Y and Terry S 2019 Opportunities and challenges for filling the air quality data gap in low- and middle-income countries *Atmos. Environ.* **215** 116794
[17] Wu S, Chen B, Webster C, Xu B and Gong P 2023 Improved human greenspace exposure equality during 21st century urbanization *Nat. Commun.* **14** 6460
[18] Jones B, O'Neill B C, McDaniel L, McGinnis S, Mearns L O and Tebaldi C 2015 Future population exposure to US heat extremes *Nat. Clim. Change* **5** 652–5
[19] Liu Z, Anderson B, Yan K, Dong W, Liao H and Shi P 2017 Global and regional changes in exposure to extreme heat and the relative contributions of climate and population change *Sci. Rep.* **7** 43909
[20] Feng S *et al* 2022 Joint exposure to air pollution, ambient temperature and residential greenness and their association with metabolic syndrome (MetS): a large population-based study among Chinese adults *Environ. Res.* **214** 113699
[21] Stevens F R, Gaughan A E, Linard C and Tatem A J 2015 Disaggregating census data for population mapping using random forests with remotely-sensed and ancillary data *PLoS One* **10** e0107042
[22] Van Donkelaar A *et al* 2021 Monthly global estimates of fine particulate matter and their uncertainty *Environ. Sci. Technol.* **55** 15287–300
[23] Abatzoglou J T, Dobrowski S Z, Parks S A and Hegewisch K C 2018 TerraClimate, a high-resolution global dataset of monthly climate and climatic water balance from 1958–2015 *Sci. Data* **5** 170191
[24] Camacho F, Cernicharo J, Lacaze R, Baret F and Weiss M 2013 GEOV1: LAI, FAPAR essential climate variables and FCOVER global time series capitalizing over existing products. Part 2: validation and intercomparison with reference products *Remote Sens. Environ.* **137** 310–29
[25] World Health Organization 2021 WHO global air quality guidelines: particulate matter ($PM_{2.5}$ and PM10), ozone, nitrogen dioxide, sulfur dioxide and carbon monoxide (World Health Organization)
[26] Health Effects Institute 2022 The state of air quality and health impacts in Africa by institute for health metrics and evaluation—Issuu (available at: www.healthdata.org/research-analysis/library/air-quality-and-health-cities)
[27] Yu W *et al* 2023 Global estimates of daily ambient fine particulate matter concentrations and unequal spatiotemporal distribution of population exposure: a machine learning modelling study *Lancet Planet. Health* **7** e209–18
[28] Lindsey R and Dahlman L 2020 Climate change: global temperature (Climate. Gov.) p 16
[29] Busby J W, Cook K H, Vizy E K, Smith T G and Bekalo M 2014 Identifying hot spots of security vulnerability associated with climate change in Africa *Clim. Change* **124** 717–31
[30] Ceccherini G, Russo S, Ameztoy I, Marchese A F and Carmona-Moreno C 2017 Heat waves in Africa 1981–2015, observations and reanalysis *Nat. Hazards Earth Syst. Sci.* **17** 115–25
[31] Stagge J H, Tallaksen L M, Gudmundsson L, Van Loon A F and Stahl K 2015 Candidate distributions for climatological drought indices (SPI and SPEI) *Int. J. Climatol.* **35** 4027–40
[32] Rentschler J, Salhab M and Jafino B A 2022 Flood exposure and poverty in 188 countries *Nat. Commun.* **13** 3527
[33] Smith A, Bates P D, Wing O, Sampson C, Quinn N and Neal J 2019 New estimates of flood exposure in developing countries using high-resolution population data *Nat. Commun.* **10** 1814
[34] Li M, Zhou -B-B, Gao M, Chen Y, Hao M, Hu G and Li X 2022 Spatiotemporal dynamics of global population and heat exposure (2020–2100): based on improved SSP-consistent population projections *Environ. Res. Lett.* **17** 094007
[35] Huang Z, Xu X, Ma M and Shen J 2022 Assessment of NO_2 population exposure from 2005 to 2020 in China *Environ. Sci. Pollut. Res.* **29** 80257–71
[36] Chen H, Sun J and Li H 2020 Increased population exposure to precipitation extremes under future warmer climates *Environ. Res. Lett.* **15** 034048
[37] Gaita S M, Boman J, Gatari M J, Pettersson J B and Janhäll S 2014 Source apportionment and seasonal variation of PM 2.5 in a Sub-Saharan African city: Nairobi, Kenya *Atmos. Chem. Phys.* **14** 9977–91
[38] Malik S, Iqbal A, Imran A, Usman M, Nadeem M, Asif S and Bokhari A 2021 Impact of economic capabilities and population agglomeration on PM 2.5 emission: empirical evidence from sub-Saharan African countries *Environ. Sci. Pollut. Res.* **28** 34017–26
[39] Naidja L, Ali-Khodja H and Khardi S 2018 Sources and levels of particulate matter in North African and Sub-Saharan cities: a literature review *Environ. Sci. Pollut. Res.* **25** 12303–28
[40] Rushingabigwi G, Nsengiyumva P, Sibomana L, Twizere C and Kalisa W 2020 Analysis of the atmospheric dust in Africa: the breathable dust's fine particulate matter $PM_{2.5}$ in correlation with carbon monoxide *Atmos. Environ.* **224** 117319
[41] Zhou L, Wu T, Pu L, Meadows M, Jiang G, Zhang J and Xie X 2023 Spatially heterogeneous relationships of $PM_{2.5}$ concentrations with natural and land use factors in the Niger River Watershed, West Africa *J. Clean. Prod.* **394** 136406
[42] Amegbor P M, Borges S S, Pysklywec A and Sabel C E 2022 Effect of individual, household and regional socioeconomic factors and $PM_{2.5}$ on anaemia: a cross-sectional study of sub-Saharan African countries *Spat. Spatio-temporal Epidemiol.* **40** 100472
[43] Li J, Han X, Jin M, Zhang X and Wang S 2019 Globally analysing spatiotemporal trends of anthropogenic $PM_{2.5}$ concentration and population's $PM_{2.5}$ exposure from 1998 to 2016 *Environ. Int.* **128** 46–62
[44] Serdeczny O, Adams S, Baarsch F, Coumou D, Robinson A, Hare W, Schaeffer M, Perrette M and Reinhardt J 2017 Climate change impacts in Sub-Saharan Africa: from physical changes to their social repercussions *Reg. Environ. Change* **17** 1585–600

[45] Tadesse W, Bishaw Z and Assefa S 2019 Wheat production and breeding in Sub-Saharan Africa: challenges and opportunities in the face of climate change *Int. J. Clim. Change Strateg. Manage.* **11** 696–715
[46] Cairns J E, Hellin J, Sonder K, Araus J L, MacRobert J F, Thierfelder C and Prasanna B M 2013 Adapting maize production to climate change in sub-Saharan Africa *Food Secur.* **5** 345–60
[47] Lottering S, Mafongoya P and Lottering R 2021 Drought and its impacts on small-scale farmers in sub-Saharan Africa: a review *South Afr. Geogr. J.* **103** 319–41
[48] Gizaw M S and Gan T Y 2017 Impact of climate change and El Niño episodes on droughts in sub-Saharan Africa *Clim. Dyn.* **49** 665–82
[49] Hyland M and Russ J 2019 Water as destiny–the long-term impacts of drought in sub-Saharan Africa *World Dev.* **115** 30–45
[50] Brandt M, Rasmussen K, Peñuelas J, Tian F, Schurgers G, Verger A, Mertz O, Palmer J R and Fensholt R 2017 Human population growth offsets climate-driven increase in woody vegetation in sub-Saharan Africa *Nat. Ecol. Evol.* **1** 0081
[51] Wei X, Liu Y, Qi L, Chen J, Wang G, Zhang L and Liu R 2023 Monitoring forest dynamics in Africa during 2000–2020 using a remotely sensed fractional tree cover dataset *Int. J. Digit. Earth* **16** 2212–32
[52] Rudel T K 2013 The national determinants of deforestation in sub-Saharan Africa *Phil. Trans. R. Soc. B* **368** 20120405
[53] Li X, Stringer L C and Dallimer M 2022 The role of blue green infrastructure in the urban thermal environment across seasons and local climate zones in East Africa *Sustain. Cities Soc.* **80** 103798
[54] Diener A and Mudu P 2021 How can vegetation protect us from air pollution? A critical review on green spaces' mitigation abilities for air-borne particles from a public health perspective-with implications for urban planning *Sci. Total Environ.* **796** 148605
[55] Zhang J, Yu Z, Zhao B, Sun R and Vejre H 2020 Links between green space and public health: a bibliometric review of global research trends and future prospects from 1901 to 2019 *Environ. Res. Lett.* **15** 063001
[56] Adenuga K I, Mahmoud A S, Dodo Y A, Albert M, Kori S A and Danlami N J 2021 Climate change adaptation and mitigation in sub-Saharan African countries *Energy and Environmental Security in Developing Countries* (Springer) pp 393–409
[57] Ikeme J 2003 Climate change daaptational deficiencies in developing countries: the case of Sub-Saharan Africa *Mitig. Adapt. Strateg. Glob. Change* **8** 29–52
[58] Bu X, Xie Z, Liu J, Wei L, Wang X, Chen M and Ren H 2021 Global $PM_{2.5}$-attributable health burden from 1990 to 2017: estimates from the global burden of disease study 2017 *Environ. Res.* **197** 111123
[59] Codjoe S N and Atiglo D Y 2020 The implications of extreme weather events for attaining the sustainable development goals in sub-Saharan Africa *Front. Clim.* **2** 592658